International Journal of Modern Physics B
Vol. 22, Nos. 9, 10 & 11 (2008) 1686–1691

World Scientific
www.worldscientific.com

SHOCK COMPACTION OF Gd-DOPED CERIA CERAMICS

HA NEUL KIM and DO KYUNG KIM

Department of Material Science and Engineering, Korea Advanced Institute of Science and Technology(KAIST), Guseoung-dong, Yuseong-gu 373-1, Daejeon, 305-701, Korea
joeperry@kaist.ac.kr

SOON NAM CHANG

Agency for Defense Development,
Yuseong P.O. Box 35-1, Daejeon, 305-600, Korea
snchang33@hanmail.net

NARESH N. THADHANI

School of Materials Science and Engineering, Georgia Institute of Technology,
Atlanta, Georgia 30332-0245, United States of America
naresh.thadhani@mse.gatech.edu

Gd-doped ceria nano powder(~5 nm) was shock-loaded by a plate impact experiment using a single stage light gas gun. A computational model was used to simulate the shock state(pressure and density changes along time) of the sample in two dimensional Eulerian code. The predicted density of compacted sample from the simulation was about 90%. To reveal the effect of shock compaction on sintering behavior, the recovered sample was heat-treated and the microstructure was compared with that of a conventionally compacted and heat-treated sample.

Keywords: Shock compaction; Gd-doped ceria; plate impact.

1. Introduction

Shock compaction has been investigated in order to obtain highly dense crack-free materials containing different properties with conventionally fabricated ones.[1-3] Some theoretical models for shock states of powders during the propagation of a shock wave were developed.[4-9] Other models described the deformation of each powder particle under a shock-loading condition.[10] Recently, two dimensional Eulerian codes were used to estimate the plastic deformation and thermal conduction among particles.[5, 11-13] These models are very important to estimate the energy state and other shock parameters affecting the shock compaction.

There exist two major problems in shock compaction. One is cracking of the compacted samples, and the other is non-uniform microstructure and mechanical properties. It was suggested that small particles have a potential to obtain crack-free compacts, because the pore size of final compacts is dependent on the particle size. And it is also considered that more uniform microstructure can be revealed because the time of shock rise seems to be enough to conduct the heat through the whole particle. Therefore

shock compaction and recovery experiment is considered as a novel technique for consolidation of nanocrystalline ceramics without grain growth.

There are a few experimental methods to obtain a shock-loaded powder compact. Some of them are explosively driven devices and others are gun systems. In case of the former, the high shock pressure is obtained by detonating explosives. In gun systems, a flyer plate accelerated by using light gas, explosives, or electromagnetic devices impacts a target sample. The principal advantages of gun systems are the reproducibility and the planarity and parallelism at impact.[4]

Gd-doped Ceria (CGO) electrolyte is one of the promising alternative electrolyte for intermediate-temperature solid-oxide fuel cell (IT-SOFC) due to their high ionic conductivity.[14, 15] It is an interesting issue whether the nanocrystals of bulk ceramics improve the ionic conductivity or not.

2. Experimental Procedure

CGO nano powder(~ 5 nm, Nextech, USA) was used. Firstly, it was statically compacted to determine the crush-strength which was theoretically developed by Fischmeister and Artz. Using the determined crush-strength and the Hugoniot data from LASL, a simulation was conducted to estimate the required velocity of the flyer plate to obtain highly dense powder compact using the two dimensional Eulerian code of Autodyn.
According to the result of simulation, a stainless steel(SS304) flyer plate was used and the velocity of projectile was determined as ~1000 m/s. The powder was pressed into a stainless steel(SS304) capsule to form a ~2 mm thick disk of 12 mm diameter at a density of 48 % of theoretical maximum density. Then the 80-mm diameter, 10-m long single stage light gas gun at Georgia Tech was used for performing the shock compaction experiment. The velocity was measured using 4 in-line shorting-pins. After the shock-loading, the steel capsule was recovered and lathed carefully to get the compacted sample out.

Pieces of recovered compact were heat-treated at 600, 700, and 800°C for 1hr. The heating and cooling rate was 120°C/hr. The heat-treated pieces were mounted and carbon-coated and then the microstructures were observed using SEM(Philips XL-30, Netherlands). The fracture surfaces of heat-treated samples were also observed and compared with the as-received one.

3. Results and Discussions

3.1. *Crush-strength determination*

The crush strength of CGO nano powder was determined from static compaction experiment. The equation based on the Fischmeister-Artz model was used to fit.[16]

$$P_y = 2.97\rho^2\left(\frac{\rho-\rho_0}{1-\rho_0}\right)\sigma_y$$

ρ_0 is initial packing density, σ_y is the yield strength of the powder, P_y is the applied pressure, and ρ is a certain final density. The determined crush strength was ~ 8 GPa from the fitted data of Fig. 1.

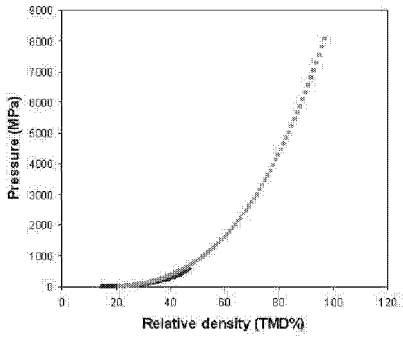

Fig. 1. Fitting data from static compaction of Gd-doped ceria.

3.2. *Simulation of the shock states of powder*

To predict the shock state of compact, numerical simulations were performed. The initial configuration used in the simulations is shown Fig. 2(a). Compaction was accomplished by introducing a compressive stress wave into the powder capsule using a gas-accelerated flyer plate.(Fig. 2(b) and (c))

The material response was simulated using the two dimensional Eulerian code Autodyn. The P-α model, which was developed by Herrman and Carrol and Holt[17-18], was used to describe the shock pressure and density of compact. Table 1 lists the values used for the material properties.

Table 1. Shock parameters of Gd-doped ceria (CGO).

Shock parameters	Gd-doped ceria (CGO)
Reference density (g/cm^3)	7.3
Porous density (g/cm^3)	3.504 (48% TMD)
Porous soundspeed (km/s)	0.21
Initial compaction P. (GPa)	0.8
Solid compaction P. (GPa)	8.069
Compaction coefficient	2.0
Gruneisen coefficient	1.40
C_0 (km/s)	4.048
S_1	1.20

To approximately determine the appropriate stress wave conditions for successful compaction, a few of simulations were performed at varying projectile impact velocities.

As a result of the simulation, the projectile velocity was determined as ~ 1000m/s which was able to compact the CGO powder over 90 % TMD.

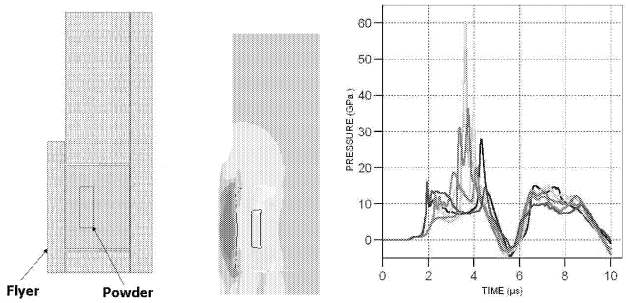

(a) (b) (c)

Fig. 2. The schematic of the simulated fixture using Autodyn. (a) before impact (b) during impact (c) time-pressure curve of the powder.

3.3. *Shock- compacted samples*

The compact was partially recovered as shown in Fig. 3(a), and a few of fragmented pieces were also obtained. The fracture surface of the as-received compact was examined using scanning electron microscope (SEM). As shown in Fig. 3(b), the grain size of as-received compact remained very small and the compact seemed to be highly dense. However, a few of microcracks existed in the compact. (Fig. 3(c))

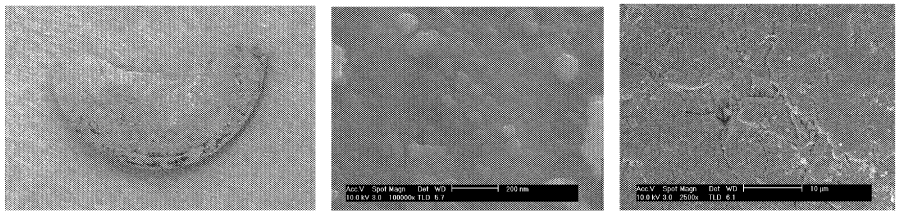

(a) (b) (c)

Fig. 3. Morphologies of as-received shock-compacted CGO. (a) recovered body (b) fracture surface (x 150,000) (c) fracture surface (x 2,500).

The fracture surfaces of heat-treated compacts from 600°C to 800°C were shown in Fig. 4. As the temperature increased, boundaries of particles became more undistinguished (Fig. 4. (d) ~ (f)), especially at 800°C. The relatively large fracture morphology also seemed to be healed from highly uniaxially-compacted structure.(Fig. 4.(a) ~ (c)) It means that the cohesion among particles starts between 700°C and 800°C. As shown Fig. 4.(g), although there were no noticeable pores at the polished surface, a few of parallel microcracks remained. It is considered that the tensile component from reflected stress wave caused to generate those cracks.

Fig. 5. shows fracture surfaces and polished surfaces of conventionally fabricated samples. They were cold-isotropically pressed(CIP) under 200 MPa and heat-treated under the same condition(600~800°C). As shown in Fig. 5.(a) ~ (c), the morphologies of fracture surfaces are different with shock-compacted samples. While the shock-compacted sample shows highly uniaxial structure, the statically-compacted sample doesn't. In Fig. 5. (d) ~ (f), there exist small pores which don't in case of shock-compacted samples. The density of CIP sample looks relatively lower compared to the shock-compacted one, and there existed a few of noticeable pores as shown in Fig. 5.(g). From the result, it can be considered that the shock compaction method has an advantage of consolidating powders, however, there still remains a limitation that microcracks exist in the compacted body.

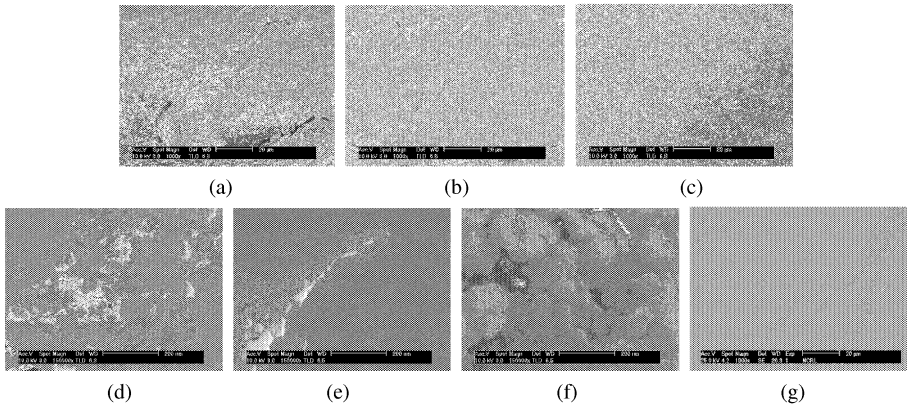

Fig. 4. Morphologies of heat-treated shock-compacted CGO. (a) 600°C (b) 700°C (c) 800°C (x 1,000) (d) 600°C (e) 700°C (f) 800°C (x 150,000) (g) polished surface (700°C).

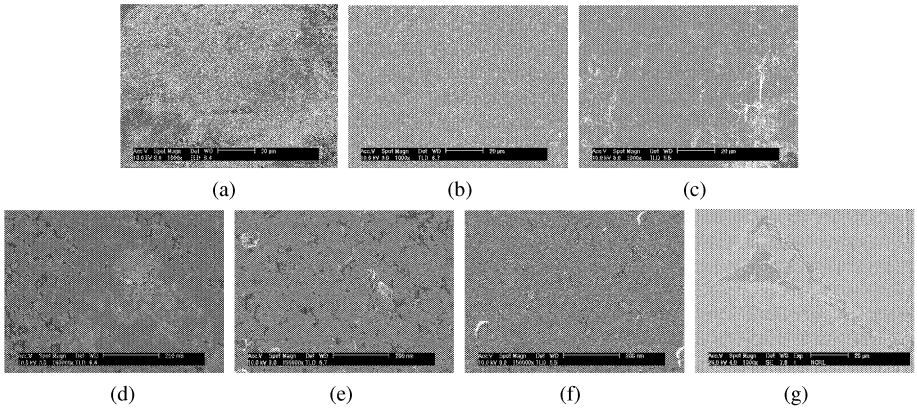

Fig. 5. Morphologies of heat-treated statically-compacted CGO. (a) 600°C (b) 700°C (c) 800°C (x 1,000) (d) 600°C (e) 700°C (f) 800°C (x 150,000) (g) polished surface (700°C).

4. Summary

The CGO nano powder was shock compacted using a plate impactor. A static compaction experiment and a simulation with a two dimensional Eulerian code were used to predict the projectile velocity for the appropriate pressure of compaction. An apparently dense body of CGO was obtained from the shock compaction. Microstructures (the fracture surface and the polished surface) of the heat-treated samples were compared to those of the conventionally fabricated ones, and there was a large microstructural difference between them. The shock-compacted body was denser than the conventionally fabricated one, however, there still existed a few of microcracks due to tensile stress component. Although it is necessary to improve some problems such as microcracks, the shock compaction method has a potential to obtain crack-free materials with novel properties.

Acknowledgments

This work was supported by Defense Acquisition Program Administration and Agency for Defense Development under the contract UD060006AD.

References

1. T. Akashi and A. B. Sawaoka, *Journal of American Ceramic Society*, 69 [4], pp. C78-80 (1986).
2. K. Kondo and S. Sawai, *Journal of American Ceramic Society*, 73 [7], pp. 1983-91 (1990).
3. Z.Q. Jin, N.N. Thadhani, M. McGill, Y. Ding, Z.L. Wang, M. Chen, H. Zeng, V.M. Chakka and J.P. Liu, *Journal of Materials Research*, 20 [3] pp. 599-609 (2005).
4. M.A. Meyers, *Dynamic Behavior of Materials* (John Wiley & Sons, INC., 1994),
5. M.A. Meyers, D.J. Benson and E.A. Olevsky, *Acta Materillia*, 47 [7], pp. 2089-2108 (1999).
6. S.R. Cooper, D.J. Benson and V.F. Nesterenko, *International Journal of Plasticity*, 16, pp. 525-540 (2000).
7. W.H. Gourdin, *Journal of Applied Physics*, 55 [1], pp. 172-181 (1984).
8. D.K. Dijken and J. Th. M. De Hosson, *Journal of Applied Physics*, 75 [1], pp. 203-209 (1994).
9. K.H. Oh and P. Persson, *Journal of Applied Physics*, 66 [10], pp. 4736-4742 (1989).
10. P. Boogerd, H.J. Verbeek, M. Stuivinga, A.C. Van der Steen and J. Schoonman, *Journal of Applied Physics*, 77 [10], pp. 5077-5085 (1995).
11. R.L. Williamson, *Journal of Applied Physics*, 68 [3], pp. 1287-1296 (1990).
12. D.J. Benson, *Modelling Simulation of Material Science and Engineering*, 2, pp. 535-550 (1994).
13. J.P. Borg, J.R. Cogar, A. Lloyd, A. Ward, D. Chapman, K. Tsembelis and W.G. Proud, *International Journal of Impact Engineering*, 33, pp. 109-118 (2006).
14. B.C.H. Steele and A. Heinzel, *Nature*, 414, pp. 345-352 (2001).
15. S.H. Jo, J.H. Kim and D.K. Kim, *Materials Science Forum*, 539-543, pp. 1373-1378 (2007).
16. H.F. Fischmeister and E. Arzt, *Powder Metallurgy*, 26 [2], pp. 82-88 (1983).
17. W. Herrmann, *Journal of Applied Physics*, 40 [6], pp. 2490-2499 (1969).
18. M. Carrol and A.C. Holt, *Journal of Applied Physics*, 43 [4], pp. 1626-1636 (1972).